


Skin depletion of *Kif3a* resembles the pediatric atopic dermatitis transcriptome profile

Mariana L. Stevens, Tesfaye B. Mersha , Zhonghua Zhang, Arjun Kothari and Gurjit K. Khurana Hershey*

Division of Asthma Research, Cincinnati Children's Hospital Medical Center, Department of Pediatrics, University of Cincinnati, Cincinnati, OH, USA

*To whom correspondence should be addressed at: Asthma Research, Cincinnati Children's Hospital Medical Center, 3333 Burnet Ave. MLC 7037, Cincinnati, OH 45229, USA. Tel: (513)636-7054; Fax: (513)636-1657; Email: Gurjit.Hershey@cchmc.org

Abstract

Skin deficiency of kinesin family member 3A causes disrupted skin barrier function and promotes development of atopic dermatitis (AD). It is not known how well *Kif3a*^{K14Δ/Δ} mice approximate the human AD transcriptome. To determine the skin transcriptomic profile of *Kif3a*^{K14Δ/Δ} mice and compare it with other murine AD models and human AD, we performed RNA-seq of full-thickness skin and epidermis from 3- and 8-week-old *Kif3a*^{K14Δ/Δ} mice and compared the differentially expressed genes (DEGs) with transcriptomic datasets from mite-induced NC/Nga, flaky tail (*Tmem79*^{ma/ma} *Flg*^{fl/fl}), and filaggrin-mutant (*Flg*^{fl/fl}) mice, as well as human AD transcriptome datasets including meta-analysis derived atopic dermatitis [MADAD] and the pediatric atopic dermatitis [PAD]. We then interrogated the *Kif3a*^{K14Δ/Δ} skin DEGs using the LINGS-L1000 database to identify potential novel drug targets for AD treatment. We identified 471 and 901 DEGs at 3 and 8 weeks of age, respectively, in the absence of *Kif3a*. *Kif3a*^{K14Δ/Δ} mice had 3.5–4.5 times more DEGs that overlapped with human AD DEGs compared to the flaky tail and *Flg*^{fl/fl} mice. Further, 55%, 85% and 75% of 8-week *Kif3a*^{K14Δ/Δ} DEGs overlapped with the MADAD and PAD non-lesional and lesional gene lists, respectively. *Kif3a*^{K14Δ/Δ} mice spontaneously develop a human AD-like gene signature, which better represents pediatric non-lesional skin compared to other mouse models including flaky tail, *Flg*^{fl/fl} and NC/Nga. Thus, *Kif3a*^{K14Δ/Δ} mice may model pediatric skin that is a precursor to the development of lesions and inflammation, and hence may be a useful model to study AD pathogenesis.

Introduction

Atopic dermatitis (AD) is the most chronic inflammatory skin disorder that affects 20% of children and 5% of adults at costs that can be close to \$5 billion every year (1). Although up to 70% present a spontaneous remission before adolescence, the presence of this disease develops into other allergic complications later in life. In fact, a systematic review found that one in every three children with AD have a risk of developing asthma in their first 4 years of life (2). A disrupted skin barrier and exacerbated immune response are important factors in this 'atopic march', however the mechanisms behind disease emergence, persistency and severity remain to be elucidated. Given the multitude of contributing factors including skin barrier disruption, exacerbated Th2 responses, and others, current animal models of AD are often not able to accurately mimic the complexities of AD and the mechanistic prelude to the atopic march. A recent study evaluated the transcriptomic profiles of six common murine models and determined how they relate to human AD skin (3). They found that no single murine model fully captures all aspects of the human AD profile. Recently, we found that the gene encoding kinesin family member 3A, *KIF3A*, is essential for skin barrier homeostasis whereby decreased *KIF3A* skin expression causes disrupted skin barrier function and promotes development of AD (4). *Kif3a*, required for the

formation of both motile and non-motile primary and sensory cilia (5,6), has been associated with AD, asthma and the atopic march by numerous studies (7–13). *KIF3A* is positioned in the 5q31 region that contains the cytokine cluster including *IL4* and *IL13*. Although null *Kif3a* mice are embryonic lethal, we and others have shown that lung-specific deletion results in a dysregulation of the Th2 allergen response, which contributes to pulmonary pathology (14–16). In mice, skin-specific deletion of *Kif3a* results in higher baseline TEWL, thicker epidermis, and disrupted expression of junctional genes. Upon epicutaneous exposure to *Aspergillus fumigatus*, *Kif3a*^{K14Δ/Δ} mice developed an exaggerated AD-like phenotype compared to K14 sufficient mice with increased transepidermal water loss and epidermal thickness, further supporting *Kif3a* role in skin homeostasis and AD (4). However, the mechanism by which *KIF3A* regulates the skin barrier remains unclear. In this study we investigated the transcriptional changes in the dermal and epidermal compartments from *Kif3a*^{K14Δ/Δ} skin at 3 and 8 weeks of age. We observed age-dependent DEGs compared to wild type mice. We then compared the identified *Kif3a*^{K14Δ/Δ} transcriptomic profiles with the publicly available transcriptomic profiles of the most common murine AD models, adult and pediatric AD transcriptomic signatures. Our studies reveal that the *Kif3*-dependent transcriptional profile overlaps with both

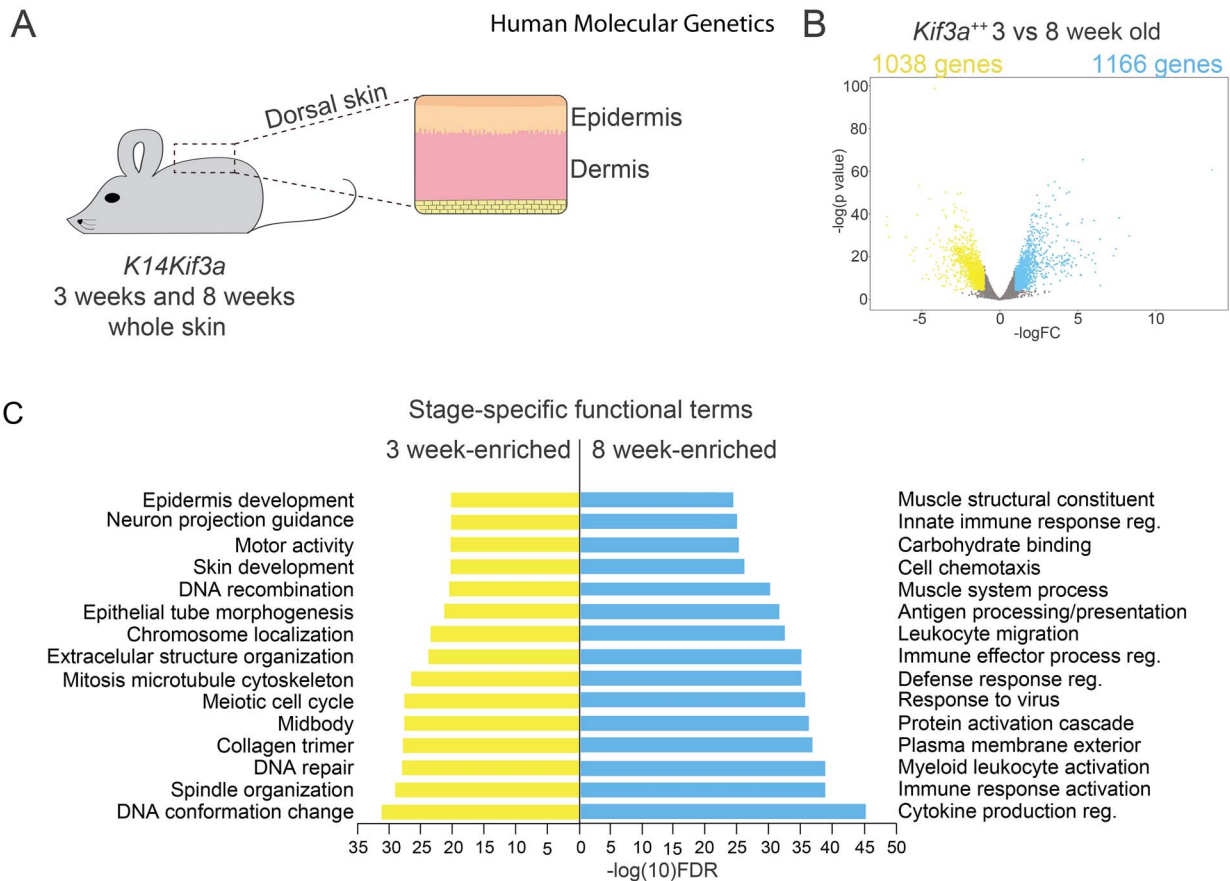


Figure 1. Transcriptional profile changes in *Kif3a*^{K14Δ/Δ} mice compared to *Kif3a*^{K14+/+} mice. **(A)** Transcriptome analysis was performed on full skin biopsies of *Kif3a*^{K14+/+} and *Kif3a*^{K14Δ/Δ} animals at 3 weeks old (juvenile) and 8 weeks old (young adult). **(B)** Comparison between juvenile and adult mice revealed 1038 enriched genes at 3 weeks of age and 1166 enriched genes at 8 weeks of age. **(C)** Functional annotation analysis is shown for skin from the 3-week-old (yellow) and 8-week-old mice (blue).

adult and pediatric AD profiles and better represents pediatric non-lesional skin compared to other mouse models. We then subjected *Kif3*-dependent DEGs to further analyses to identify novel potential AD target pathways as potential therapies.

Results

Skin *Kif3a* loss of function leads to age-specific transcriptional profile changes

Kif3a^{K14Δ/Δ} mice have disrupted skin barrier function with significantly higher transepidermal water loss compared to their wild type counterparts (4). However, the timing of *Kif3a* contribution to skin homeostasis at post-natal stages of development is not yet known. We performed transcriptome analysis on full skin biopsies of *Kif3a*^{K14+/+} and *Kif3a*^{K14Δ/Δ} animals at 3 weeks old (juvenile) and 8 weeks old (young adult) (Fig. 1A). To address baseline developmental differences in the skin between juvenile and adult mice, we first compared 3- and 8-week-old wild type mice. This analysis reveals 1038 DEGs at 3 weeks of age and 1166 DEGs at 8 weeks of age (Fig. 1B). Functional annotation analysis reveals that the juvenile skin profile has a strong skin development

and skin proliferation signature, demonstrated by related terms, such as epithelial tube morphogenesis, chromosome localization, midbody, spindle organization, epidermis development and skin development (Fig. 1C—yellow). Weeks later, the skin develops a marked immune response signature where both innate and adaptive immune response genes are represented by terms such as innate immune response regulation, antigen processing and presentation, leukocyte migration, response to virus, and cytokine production (Fig. 1C—blue).

We next compared *Kif3a*^{K14Δ/Δ} and *Kif3a*^{K14+/+} at 3 and 8 weeks of age. We identified 471 DEGs at 3 weeks of age, including 286 downregulated and 185 upregulated genes and 901 DEGs at 8 weeks of age including 230 downregulated and 671 upregulated genes (Fig. 2A). A comparison of both DEG datasets shows that 70% (330/471) of 3-weeks DEGs are unique to this stage, whereas 84% (760/901) of the 8-weeks DEGs are stage-specific (Fig. 2B). A total of 141 DEGs are shared in both datasets, which includes all *Kif3a*-dependent genes throughout juvenile and early adulthood stages. Among juvenile DEGs are *Shh*, *Dkk1*, *S100a8* and *S100a9*, whereas *Krt1*, *Cav3* and *Gata3* are amongst the adult DEGs. Shared

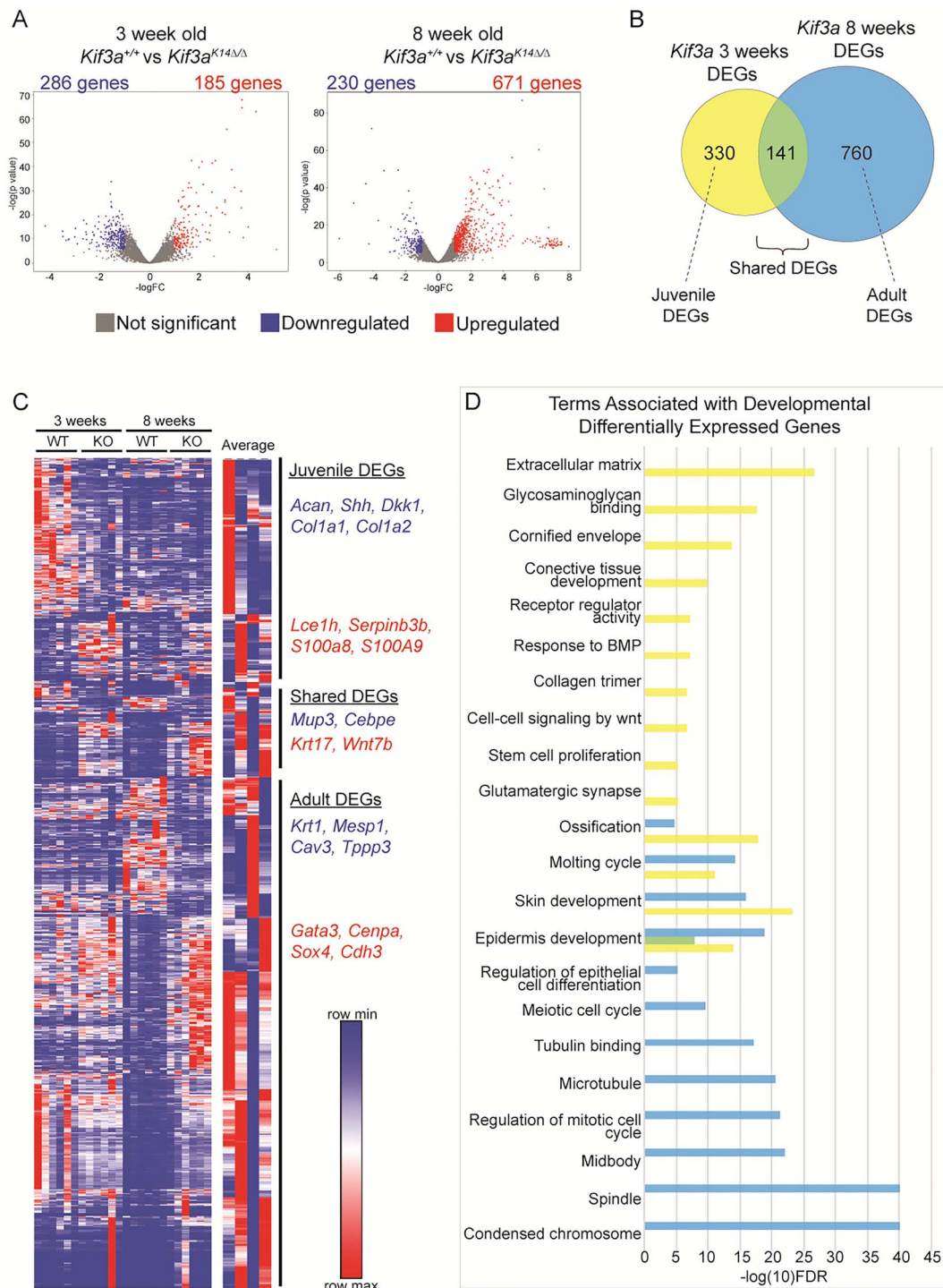


Figure 2. Comparison of *Kif3a*-dependent DEGs at 3 and 8 weeks of age. **(A)** There were 471 DEGs at 3 weeks of age, including 286 downregulated and 185 upregulated genes and 901 DEGs at 8 weeks of age including 230 downregulated and 671 upregulated genes. **(B)** Venn diagram of DEG datasets shows that 70% (330/471) of 3-week DEGs are unique to this stage, whereas 84% (760/901) of the 8-week DEGs are stage-specific. **(C)** Heatmap shows shared and distinct DEGs among juvenile and adult stages. **(D)** Functional annotation analysis of *Kif3a*-dependent genes at 3 weeks (yellow) and 8 weeks of age (blue).

DEGs across juvenile and adult stages include *Mup3*, *Krt17* and *Wnt7b* (Fig. 2C). Functional term analysis of these gene sets revealed that juvenile *Kif3a*-dependent genes are mostly components of the extracellular matrix and connective tissue, in addition to being involved with signaling activity such as BMP and Wnt pathways

(Fig. 2D—yellow). Meanwhile at 8 weeks of age, the top functional terms for the adult DEGs are related to cell division, including chromosome condensation, spindle and microtubules (Fig. 2D—blue). As expected, terms shared among datasets include epidermis and skin development (Fig. 2D). Collectively, the data support that

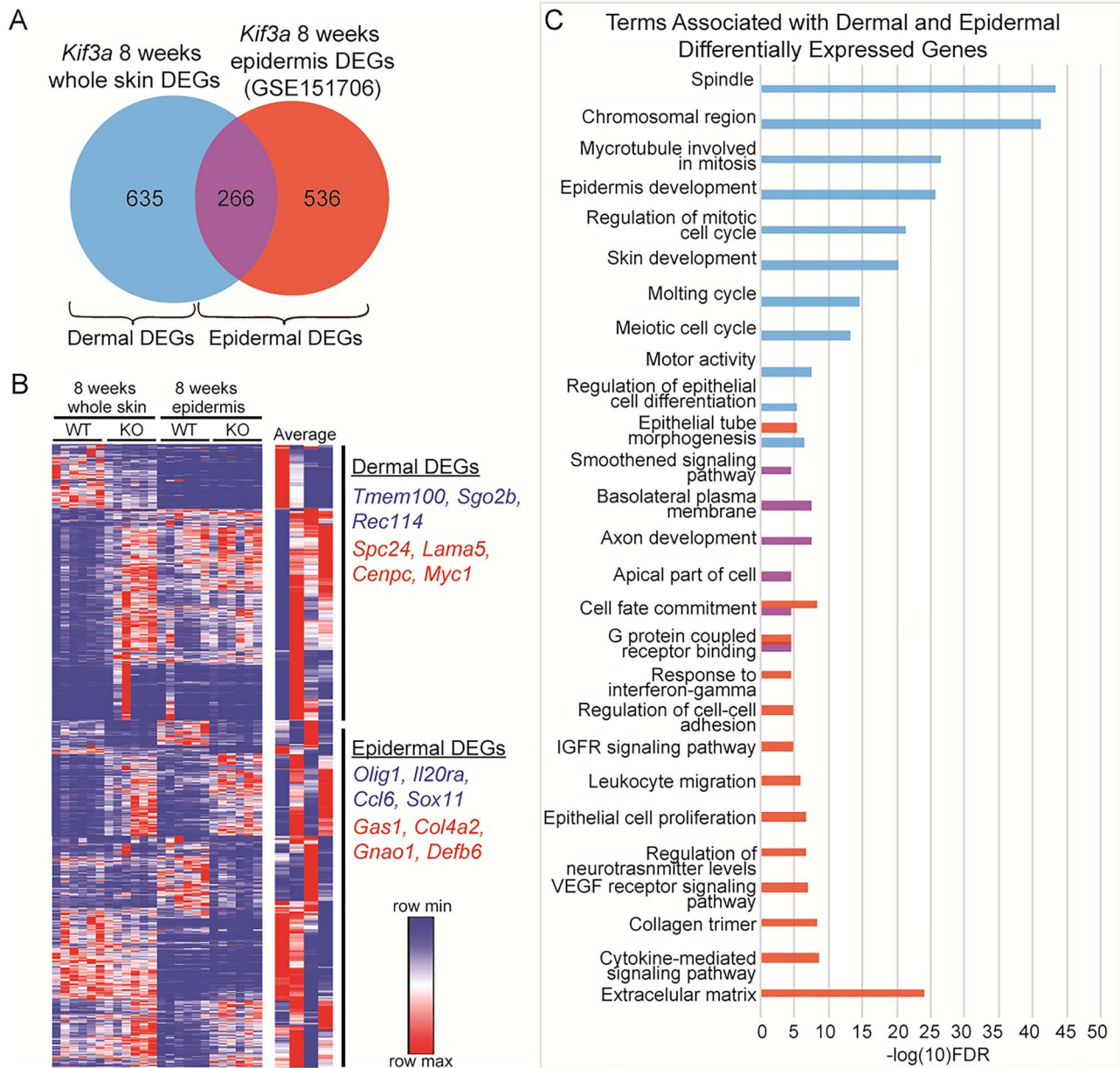


Figure 3. *Kif3a* plays distinct roles in the epidermis and dermis. (A) Venn diagram of DEGs in full-thickness skin and isolated epidermis of *Kif3a*^{K14Δ/Δ} versus *Kif3a*^{K14+/+} mice. (B) Heatmap shows shared and distinct *Kif3a*-dependent DEGs among the epidermis and dermis at 8 weeks of age. (C) Functional annotation analysis of dermal and epidermal compartment DEGs.

absence of *Kif3a* at 8 weeks switches the predominant pathways from the immune response to more of the juvenile signature including cell division and proliferation (Supplementary Material, Fig. S1).

Kif3a plays distinct roles in the epidermis and dermis

By comparing transcriptional changes in full-thickness skin and isolated epidermis of *Kif3a*^{K14Δ/Δ} mice, we found that 70% of all DEGs we observed at 8 weeks of age (635/901) were not present in the epidermal gene set (Fig. 3A). Among the 802 epidermal DEGs, only 33% of them (266/802) were also present in the full-thickness dataset. The small coverage of epidermal transcriptional changes seen in the full-thickness samples is likely

due to dilution by the much thicker dermal layer (Fig. 1A). Among the dermal DEGs are *Tmem100*, *Sgo2b*, *Spc24* and *Lama5*, whereas the epidermal DEGs include *Olig1*, *Il20ra*, *Gas1* and *Defb6* (Fig. 3B). Functional term analysis revealed dermal DEGs to be involved in cell division, whereas the epidermal compartment signature functions include cell adhesion and a variety of cell signaling branches such as G protein, interferon-gamma, IGFR and VEGF (Fig. 3C).

Skin *Kif3a* deficiency features pediatric and adult AD transcriptome profiles

Disrupted skin barrier and increased TEWL, as seen in the *Kif3a* animals, are hallmarks of AD (4). We used publicly available data to assess how much of the transcriptional

Table 1. Demographics of the adult and pediatric atopic dermatitis cohort populations included in the present study

	Pediatric AD skin	Pediatric control skin	MADAD
	n = 19	n = 18	n = 56
Age mean (SD)	1.3 (1.2)	1.2 (0.8)	45.17 (30.17)
Male sex (%)	11 (57.9%)	8 (44.4%)	NA
Black race (%)	5 (26.3%)	1 (5.6%)	NA
IgE total: kU/L (mean, SD)	1290.4 (1798.2)	NA	NA
SCORAD total (mean, SD)	57.8 (12.8)	NA	>25
EASI total (mean, SD)	12.7 (6.9)	NA	>12
Pruritus ADQ (mean, SD)	16.8 (9.1)	NA	NA
TEWL lesional g/m ² /h (mean, SD)	32.1 (14.0)	NA	NA
TEWL non-lesional g/m ² /h (mean, SD)	16.1 (8.0)	NA	NA

Abbreviations: AD, atopic dermatitis; EASI, Eczema Area and Severity Index; IgE, immunoglobulin E; NA, not assessed; SCORAD, SCORing Atopic Dermatitis; SD, standard deviation; TEWL, transepidermal water loss.

changes observed in *Kif3a*^{K14Δ/Δ} mice are shared by other mouse AD models and by human AD transcriptomes. We focused on the three major published animal models of AD: mite-induced NC/Nga (17,18), flaky tail (*Tmem79*^{ma/ma} *Flg*^{fl/fl}) (19,20), *Flg*-mutated (*Flg*^{fl/fl}) (21); and two publicly available human AD transcriptome datasets: the meta-analysis derived atopic dermatitis (MADAD) (22) and the pediatric AD dataset (23) (Fig. 4A and B). The murine models include adult animals at 8, 10 or 26 weeks of age, and the human transcriptome datasets span pediatric and adult AD participants ranging from 0 to 81 years old (Supplementary Material, Table S1). Heatmap of the 594 MADAD genes show similarity between adult AD profile and some of the mouse models. The 8-week *Kif3a*^{K14Δ/Δ} and mite-sensitized NC/Nga DEGs have more overlap with the human adult and pediatric non-lesional and lesional AD DEGs compared to the other mouse models (Fig. 4C and D). *Kif3a*^{K14Δ/Δ} mice have 3.5–4.5 times more DEGs that are overlapping with MADAD and pediatric DEGs than the flaky tail and *Flg*^{fl/fl} mice. Despite the larger DEG overlap observed between mite-sensitized NC/Nga model with adult AD (18%), this was not observed with the non-lesional or lesional pediatric profiles, where the DEG overlap was only 7.1% and 6.7%, respectively (Fig. 4E).

Skin *Kif3a* deficiency mimics cell cycle and epidermis development disruption present in pediatric and adult AD transcriptome profiles

Given the greater overlap of the full skin *Kif3a*^{K14Δ/Δ} 8-week-old mice with human AD compared to 3-week-old mice, the 8-week data were chosen for all further analyses. The *Kif3a*^{K14Δ/Δ} had more DEGs overlapping with pediatric AD, whereas the NC/Nga mite-sensitized model had more overlap with MADAD (Fig. 5A–C). As shown in the Venn diagrams, 55% (45/82), 85% (98/115) and 75% (176/234) of 8-week *Kif3a*^{K14Δ/Δ} DEGs that overlapped with the MADAD and pediatric non-lesional and lesional gene lists, respectively, were not shared with the NC/Nga mite-sensitized model (Fig. 5A–C). Functional annotation of the common 45 genes between the *Kif3a*^{K14Δ/Δ} model and MADAD revealed them to be involved with regulation of cell division (e.g. chromosome segregation,

spindle and cell cycle G2/M phase transition) (Fig. 5A). Interestingly, the functions of the 98 and 176 DEGs overlapping between pediatric AD and *Kif3a*^{K14Δ/Δ} included not only cell cycle regulation functions, but also epidermis and skin development (Fig. 5B and C). Common DEGs between each of the AD murine models and human transcriptomes revealed a strong cell cycle signature (Supplementary Material, Fig. S2A and B). Detailed analysis of the shared transcriptional changes between adult and pediatric AD and the NC/Nga mite model revealed genes primarily involved in the inflammatory response (e.g. leukocyte migration, granulocyte activation, regulation of defense response and chemokine production) (Supplementary Material, Fig. S2C–E). Collectively, these data suggest that *Kif3a*^{K14Δ/Δ} mice resemble the human AD transcriptome profile with respect to disrupted cell cycle regulation and epidermis development, the latter of which is not present in the NC/Nga mite model. Further, *Kif3a*^{K14Δ/Δ} mice better represented pediatric non-lesional skin compared to NC/Nga mice. Thus, *Kif3a*^{K14Δ/Δ} mice may be a better model of non-lesional skin that is a precursor to the development of lesions and inflammation, and hence a useful model to study AD pathogenesis.

Cell cycle genes are potential new targets for AD

Given the strong cell cycle signature in both murine and human AD datasets, we further analyzed these DEGs. Most of the cell cycle-related DEGs were upregulated in 8-week *Kif3a*^{K14Δ/Δ} mice, as well as in the adult and pediatric lesional AD datasets (Fig. 5D). To explore drug targets that target *Kif3a*-dependent DEGs, we compared the top DEGs of 8-week-old *Kif3a*^{K14Δ/Δ} mice against the LINCS-L1000 database (lincsproject.org). The results show a total of nine compounds with negative connectivity scores of <−80, indicating that they may be likely to reverse the skin phenotype. Seven out of the nine negative scored compounds are known anti-cancer drugs (irinotecan, CD-437, pyrrvinium-pamoate, homoharringtonine, clofarabine, verrucarin-a, azacitidine), with the potential to inhibit cell cycle genes, which were upregulated in *Kif3a*^{K14Δ/Δ} mice. Our results also identified an anti-histamine drug, cyproheptadine. Anti-histamines are widely used in the treatment of

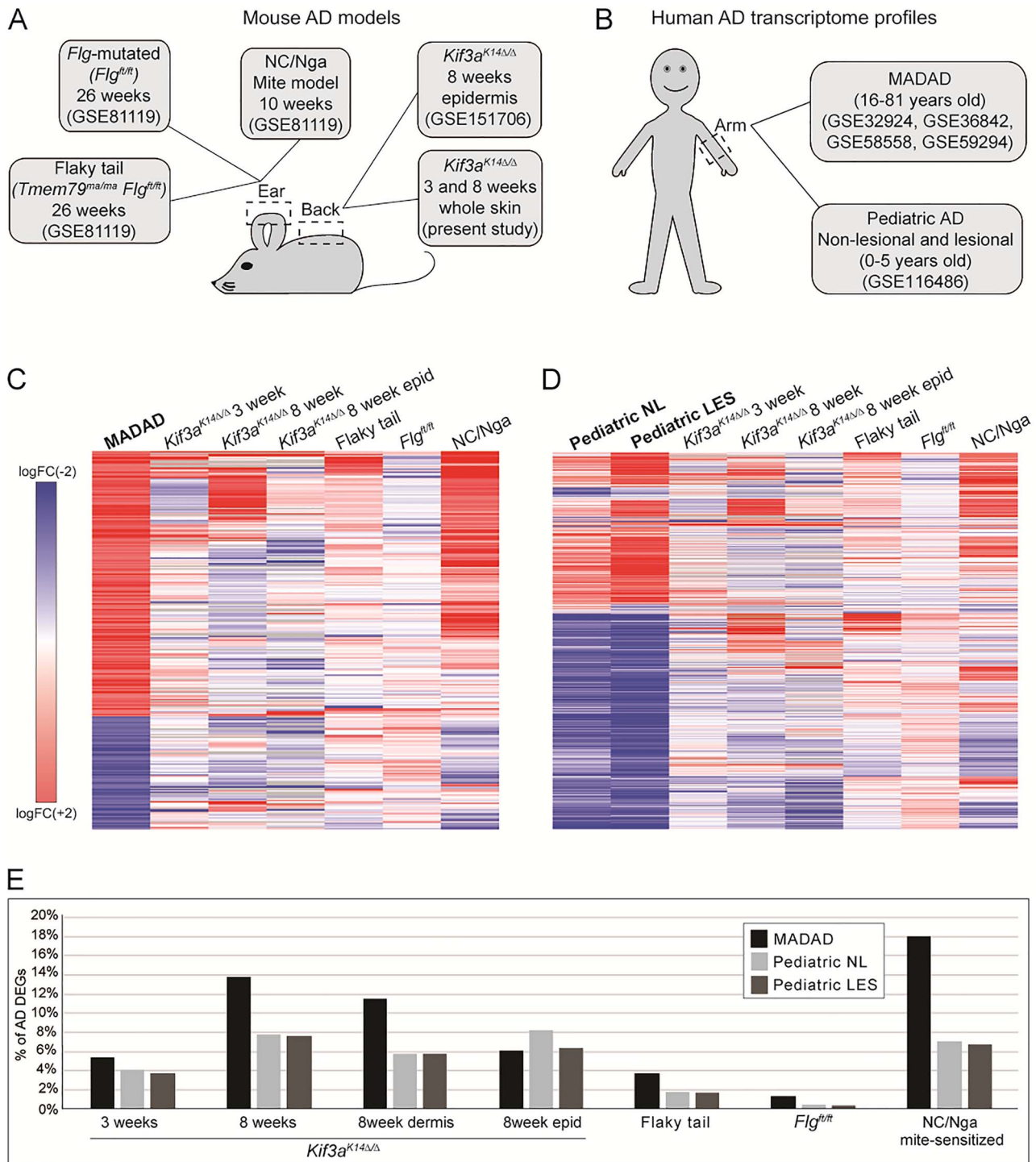


Figure 4. Comparison of the AD transcriptomic signatures in different mouse models with human pediatric and adult atopic dermatitis transcriptome profiles. **(A)** Mouse AD models and **(B)** human AD transcriptomic datasets included in this study analysis. **(C and D)** Heatmap of the comparison of the DEGs of the mouse AD models with adult and pediatric AD datasets. NL = non-lesional, LES = lesional. **(E)** Percent of DEGs in each mouse model that are overlap with human adult MADAD and pediatric NL (non-lesional) and LES (lesional) DEGs.

allergies, including AD. (24) Interestingly, the analysis also suggested a synthetic cannabinoid, HU-211, to reverse the gene expression changes upon skin disruption seen in *Kif3a^{K14Δ/Δ}* mice. HU-211 is a N-Methyl-D-aspartate receptor antagonist currently undergoing Phase I trials for the treatment of brain cancer and advanced solid tumors (25) (Fig. 5E and Supplementary Material, Table S2).

Discussion

In this study, a transcriptomics approach was used to identify differentially expressed skin genes from *Kif3a^{K14Δ/Δ}* mice and then to compare these to commonly used AD mouse models and to human adult and pediatric AD. Our findings reveal that *Kif3a^{K14Δ/Δ}* mice have 3.5 and 4.5 times more DEGs overlapping with the

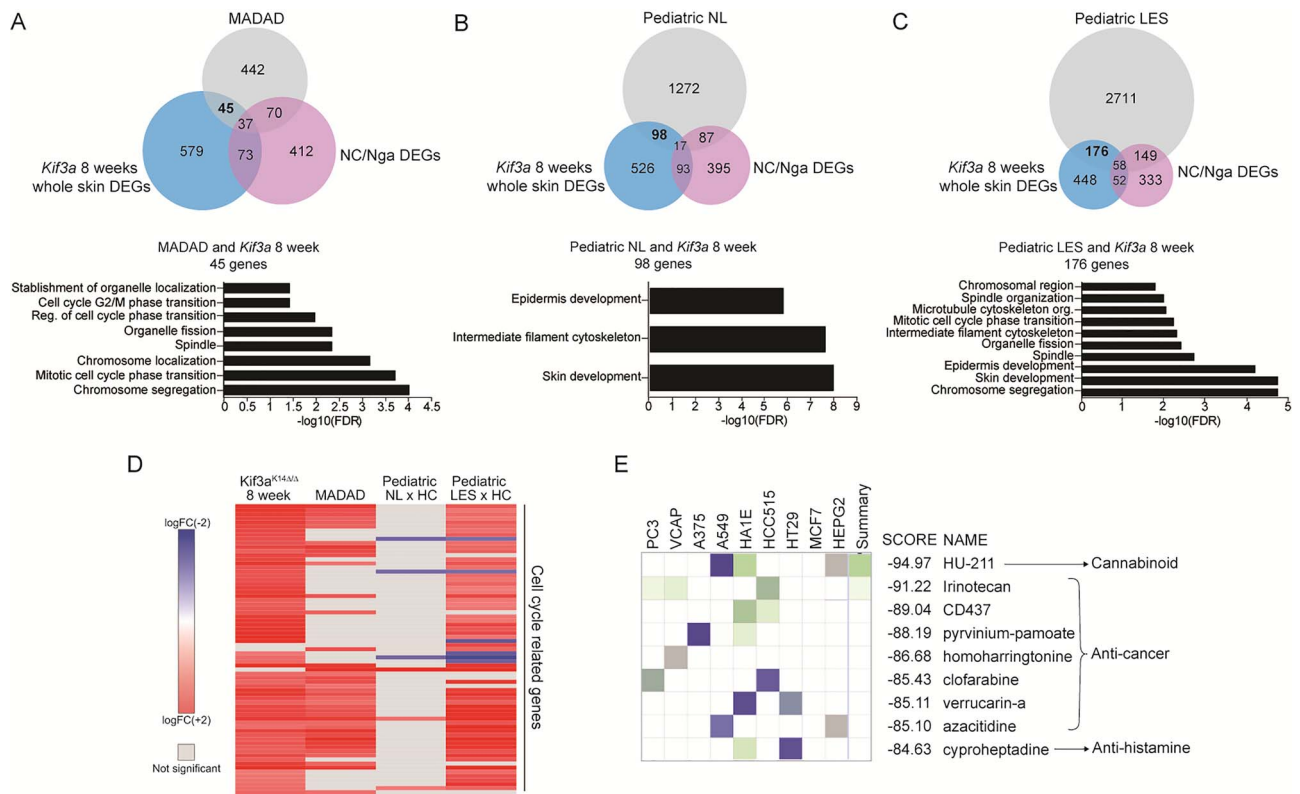


Figure 5. Skin *Kif3a* deficiency mimics cell cycle and epidermis development disruption present in pediatric and adult atopic dermatitis transcriptome profiles. (A–C) Venn diagrams and functional annotation analysis of DEGs that are distinct and common between whole skin of 8-week-old *Kif3a* deficient mice, NC/Nga mice, and human adult AD, MADAD, pediatric non-lesional skin and pediatric lesional skin. (D) Heatmap of cell cycle related DEGs dysregulated in in 8-week *Kif3a*^{K14Δ/Δ} mice, adult and pediatric lesional AD datasets. (E) LINCS-L1000 database and potential novel AD drugs that target the *Kif3a* pathway.

Table 2. Drug compounds identified using the drug discovery tool LINCS-L1000 (lincsproject.org). Connectivity scores quantify the commonality between *Kif3a*-dependent transcriptional profile and the drugs. Score of < -80 indicates opposite effects between the two datasets

Score	Name	Description	Properties
-94.97	Dexanabinol (HU-211)	Glutamate receptor antagonist	Cannabinoid
-91.22	Irinotecan	Topoisomerase inhibitor	Anti-cancer
-89.04	CD-437	Retinoid receptor agonist	Anti-cancer
-88.19	Pyrvinium-pamoate	AKT inhibitor	Anti-cancer
-86.68	Homoharringtonine	Protein synthesis inhibitor	Anti-cancer
-85.43	Clofarabine	Ribonucleoside reductase inhibitor	Anti-cancer
-85.11	Verrucarín-a	Protein synthesis inhibitor	Anti-cancer
-85.1	Azacitidine	DNA methyltransferase inhibitor	Anti-cancer
-84.63	Cyproheptadine	Histamine receptor antagonist	Anti-histamine

MADAD and pediatric DEGs, respectively, than flaky tail or *Flg^{fl/fl}* mice. The NC/Nga mite model revealed genes primarily involved in the inflammatory response, while the *Kif3a*^{K14Δ/Δ} mice better resembled the disrupted cell cycle regulation and disrupted epidermis development observed in human AD. In the absence of *Kif3a*, mice spontaneously develop an AD-like transcriptomic signature at 8 weeks of age and the epidermal changes better represent non-lesional pediatric skin compared to other mouse models. This is consistent with our previous published work demonstrating that these mice have increased TEWL without any manipulation (4). Thus, *Kif3a*^{K14Δ/Δ} mice may be a useful model of pediatric non-lesional skin that is a precursor to the development of

lesions and inflammation, and hence a useful model to study AD pathogenesis.

Kif3a^{K14Δ/Δ} mice have distinct skin transcriptomes at 3 and 8 weeks of age that contribute to the observed skin barrier defect. At 3 weeks of age, skin *Kif3a* deficiency affects important developmental signaling pathway, such as BMP and Wnt, while at 8 weeks of age skin *Kif3a* deficiency results in increased cell proliferation. Although most studies use full skin biopsies, we were able to dissect the roles of dermis and epidermis separately, revealing their individual and combined contributions to barrier homeostasis.

We found that although the dermal layer comprises a larger portion of the skin, it is within the epidermis that

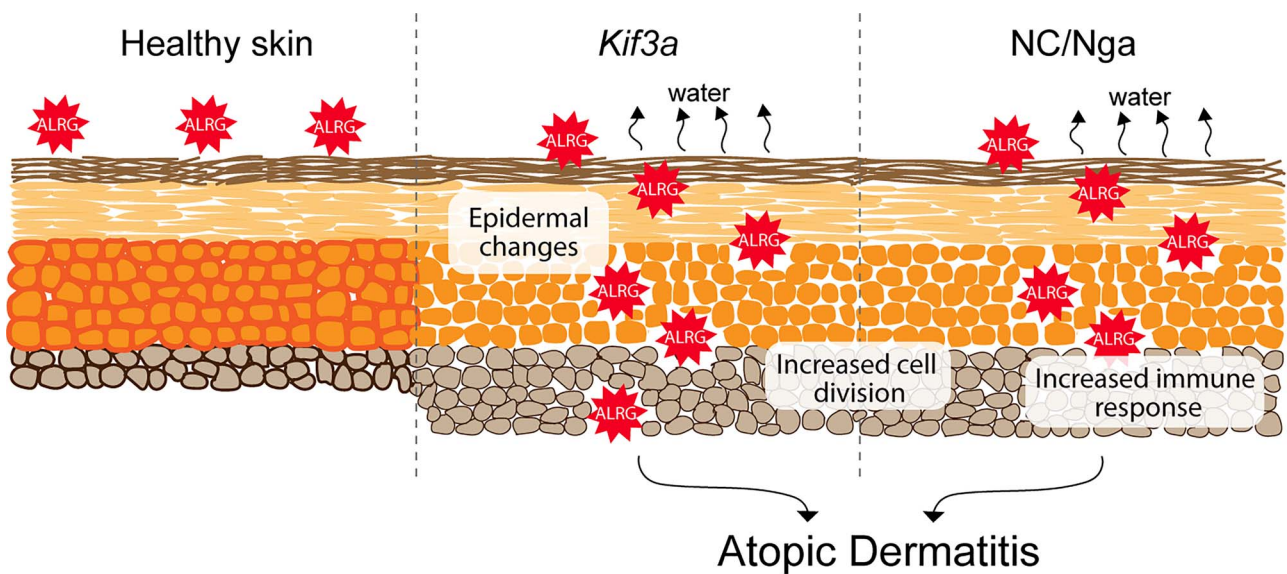


Figure 6. Skin schematic of the proposed model of the contribution of *Kif3a* to skin barrier homeostasis. *Kif3a* deficiency in the skin leads to spontaneous development of a human AD-like gene signature, which provides a model of pediatric non-lesional skin. Absence of skin *Kif3a* dysregulates genes in the epidermis and dermis impairing skin barrier function even in the absence of an underlying exacerbated immune response.

important signaling crosstalk and immune responses including cell–cell adhesion, response to interferon-gamma, and leukocyte migration are taking place. However, it is possible that our approach did not fully capture the dermal signature. When compared to human AD, skin *Kif3a* deficiency and pediatric and adult AD transcriptomes shared signatures of increased cell proliferation and disrupted epidermis development. Importantly, these signatures were not present in the mite-sensitized NC/Nga model. Further, *Kif3a*^{K14Δ/Δ} mice had considerable transcriptome overlap with pediatric non-lesional skin. They both also share skin barrier disruption as evidenced by increased TEWL in *Kif3a*^{K14Δ/Δ} mice (4) and in non-lesional skin of pediatric AD (26). Thus, the absence of skin *Kif3a* impairs proper barrier function even in the absence of an underlying exacerbated immune response, separating epidermal abnormalities from inflammation (Fig. 6). This is highly significant and highlights an opportunity to intervene and treat/prevent AD *before* there is inflammation. We analyzed the *Kif3a*-dependent DEGs using a drug discovery database in order to identify new potential AD therapies that target the *Kif3a* pathway. We found that *Kif3a* DEGs could be potentially targeted with drugs used in cancer therapy as well as the H1 antagonist cyproheptadine. The finding of the anti-cancer drugs potential candidates is interesting and may suggest an unrecognized role for *Kif3a*. There are also indication of cannabinoids to control itching and inflammatory responses (27,28), making them a great target for future studies. The ability to repurpose drug for another disease saves time and costs during a clinical trial process (29).

It is unlikely that a single gene alone is responsible for a complex disease, such as AD. Not surprisingly, the filaggrin mutant mouse model leads to only a small number of DEGs that overlap with human AD (3). In this study, we

dissected the individual contribution of *Kif3a* to AD and our findings highlight overlap with published human and pediatric AD transcriptomes and show that the overlap is greater than previously reported mouse models. We found an increased cell division signature likely responsible for the thicker epidermal skin layer seen in AD patients. Epidermal cells receive proliferation signals in detriment of epidermal differentiation contributing to defective barrier function. The *Kif3a*^{K14Δ/Δ} model, but not the mite-sensitized NC/Nga model, mimics the thicker and abnormally differentiated epidermis often seen in AD. Further, this is evident without inflammation, a common feature of AD non-lesional skin. Recently published work with human AD transcriptomes revealed that the core DEGs were not enriched for immune response and inflammation, but rather for signal transduction pathways, supporting our findings in the *Kif3a*^{K14Δ/Δ} model (30).

Comparison of *Kif3a*^{K14Δ/Δ} mice skin transcriptomes with adult lesional and non-lesional skin show that while the transcriptome from an 8-week-old *Kif3a*^{K14Δ/Δ} mouse best represents the human AD transcriptome, the dermis and epidermis have different phenotypes. The dermis more closely resembles adult skin, whereas the epidermis more closely resembles pediatric non-lesional skin. Available human datasets are all from full-thickness skin biopsies, but our data support that upon *Kif3a* loss, the epidermal layer better models non-lesional pediatric skin.

Although mouse models have significantly advanced our understanding of skin biology and diseases, there is only 30% identity between the top human and mouse skin DEGs in AD. The data reinforce that no murine model fully mimics or represents human AD. Although the NC/Nga model mimics the Th1, Th2 and Th17 immune responses, it lacks features of dysregulated

epidermal differentiation and tight junction disruption. The flaky-tail and Flg-mutated models better represent the barrier abnormalities like decreased filaggrin and loricrin, but lack the substantial Th2 immune response (3). The *Kif3a* skin deficiency model represents the non-immune features of AD such as increased TEWL, increased epidermal proliferation, increased epidermal thickness, and dysregulation of cell–cell adhesion and extracellular matrix, which best models non-lesional skin compared to other available AD mouse models (4). Our previously published work revealed that these mice are more susceptible to AD development suggesting that these mice may be useful models of non-lesional AD skin, i.e. immediate precursors of disease. Potential new therapies targeting these pathways may be beneficial for primary or secondary prevention of AD.

Materials and Methods

Generation of *Kif3a*^{K14Δ/Δ} mice with targeted deletion of *Kif3a* in the skin

Skin-specific conditional *Kif3a* knockout mice were generated by breeding K14-Cre;R26R-eYFPflox-stop-flox mice (31) to *Kif3a* flox/flox mice (32). In the presence of K14-driven Cre-recombinase, flox-flanked exon 2 of the *Kif3a* gene was deleted in epidermal cells introducing a frameshift in the coding region resulting in premature termination of *Kif3a* translation. *Kif3a*^{K14Δ/Δ} mice were maintained on an alternating 12-hour light cycle with food and water ad libitum, and otherwise maintained and handled according to the Guide for the Care and Use of Laboratory Animals (Institute of Laboratory Animal Resources, National Research Council).

Mice skin RNA isolation and quantitative real time PCR

Total RNA was isolated from homogenized mouse skin using RNeasy Microarray Tissue Mini Kit (Qiagen) according to manufactures' instructions.

RNA-seq data and analysis

Skin mRNA from *Kif3a*^{+/+} and *Kif3a*^{K14Δ/Δ} at 3 and 8 weeks of age were submitted for RNA-seq at the Genomics, Epigenomics and Sequencing Core at the University of Cincinnati. The RNA quality was determined by Bioanalyzer (Agilent, Santa Clara, CA, USA). NEBNext Poly(A) mRNA Magnetic Isolation Module (New England BioLabs, Ipswich, MA, USA) was used to isolate polyA RNA. Libraries were prepared with NEBNext Ultra II Directional RNA Library Prep Kit (New England BioLabs) and sequenced using HiSeq 1000 sequencer (Illumina, San Diego, CA, USA). Each sample had around 25 million single reads at 51 bp long. Quality trimmed reads were mapped to the mm10 genome, quantified using RSEM and mapped with Bowtie 2 using default thresholds (33).

Differential gene expression analysis was carried out with RUVSeq (34) with log₂ fold change (FC) ≥1 or

≤−1, $P < 0.05$ and false discovery rate ≤5%. Volcano Plots were generated using CSBB's Interactive Scatter Plot module. Gene ontology term enrichment analyses were performed using WebGestalt (35). Heatmaps were generated using GeneE from Broad Institute (<https://software.broadinstitute.org/GENE-E/index.html>). The whole-genome-sequencing data associated with this study will be available through GEO. Publicly available datasets used in the study are: GSE151706 (*Kif3a*^{K14Δ/Δ} 8-week epidermis), GSE81119 (Flaky tail, *Flgft/ft* (24,25) and NC/Nga mite models (22,23)), GSE32924 (MADAD), GSE36842 (MADAD), GSE58558 (MADAD), GSE59294 (MADAD) (27), GSE10736 (pediatric AD non-lesional and lesional) (28).

Connectivity Map (CMap) analysis of LINCS-L1000 data to identify potential drug targets

To explore potential drug targets that target *Kif3a*-dependent DEGs, we systematically mine and compared the top DEGs of 8-week-old *Kif3a*^{K14Δ/Δ} mice against the LINCS-L1000 database (<https://lincsproject.org/>) (36). This analysis workflow uses LINCS and Kolmogorov–Smirnov test- (KS test) based algorithm to rank candidate compounds. The associated pattern-matching software searches for two-directional matches, considering both the up and down DEG gene sets, when comparing the query against signatures (z-scored differential expressions) in the LINCS L1000 dataset. The system then generates a list of signatures rank ordered by the strength of the match to the query. CMap instance was measured by an enrichment score, which ranged from −1 to 1, and a permutation P -value. For the current analysis, any connectivity score of below −0.85 or above 0.85 was considered (37,38).

Supplementary Material

Supplementary Material is available at HMG online.

Conflict of Interest statement. None declared.

Funding

This work was supported by the National Institutes of Health (NIH) grant U19AI1070235 (G.K.K.H.) and HL132344 (T.B.M.).

Author contributions

M.L.S.: designed and performed experiments; wrote first draft of manuscript; Z.Z.: designed and performed experiments; A.K. performed the RNA-seq analyses; T.B.M. aided in RNA-seq analyses and writing the manuscript; G.K.K.H.: conceived overall experimental design and plan, writing and editing of manuscript; secured funding for the study.

References

- Weidinger, S. and Novak, N. (2016) Atopic dermatitis. *Lancet*, **387**, 1109–1122.
- van der Hulst, A.E., Klip, H. and Brand, P.L. (2007) Risk of developing asthma in young children with atopic eczema: a systematic review. *J. Allergy Clin. Immunol.*, **120**, 565–569.
- Ewald, D.A., Noda, S., Oliva, M., Litman, T., Nakajima, S., Li, X., Xu, H., Workman, C.T., Scheipers, P., Svitacheva, N. et al. (2017) Major differences between human atopic dermatitis and murine models, as determined by using global transcriptomic profiling. *J. Allergy Clin. Immunol.*, **139**, 562–571.
- Stevens, M.L., Zhang, Z., Johansson, E., Ray, S., Jagpal, A., Ruff, B.P., Kothari, A., He, H., Martin, L.J., Ji, H. et al. (2020) Disease-associated KIF3A variants alter gene methylation and expression impacting skin barrier and atopic dermatitis risk. *Nat. Commun.*, **11**, 4092.
- Hirokawa, N. (2000) Stirring up development with the heterotrimeric kinesin KIF3. *Traffic*, **1**, 29–34.
- Hirokawa, N., Noda, Y., Tanaka, Y. and Niwa, S. (2009) Kinesin superfamily motor proteins and intracellular transport. *Nat Rev Mol Cell Biol*, **10**, 682–696.
- Lepre, T., Cascella, R., Ragazzo, M., Galli, E., Novelli, G. and Giardina, E. (2013) Association of KIF3A, but not OVOL1 and ACTL9, with atopic eczema in Italian patients. *Br. J. Dermatol.*, **168**, 1106–1108.
- Hirota, T., Takahashi, A., Kubo, M., Tsunoda, T., Tomita, K., Sakashita, M., Yamada, T., Fujieda, S., Tanaka, S., Doi, S. et al. (2012) Genome-wide association study identifies eight new susceptibility loci for atopic dermatitis in the Japanese population. *Nat. Genet.*, **44**, 1222–1226.
- Kim, M., Suh, Y.A., Oh, J.H., Lee, B.R., Kim, J. and Jang, S.J. (2017) Corrigendum: KIF3A binds to beta-arrestin for suppressing Wnt/beta-catenin signalling independently of primary cilia in lung cancer. *Sci. Rep.*, **7**, 46773.
- Kovacic, M.B., Myers, J.M., Wang, N., Martin, L.J., Lindsey, M., Ericksen, M.B., He, H., Patterson, T.L., Baye, T.M., Torgerson, D. et al. (2011) Identification of KIF3A as a novel candidate gene for childhood asthma using RNA expression and population allelic frequencies differences. *PLoS One*, **6**, e23714.
- Michel, S., Liang, L., Depner, M., Klopp, N., Ruether, A., Kumar, A., Schedel, M., Vogelberg, C., von Mutius, E., von Berg, A. et al. (2010) Unifying candidate gene and GWAS approaches in asthma. *PLoS One*, **5**, e13894.
- Johansson, E., Biagini Myers, J.M., Martin, L.J., He, H., Pilipenko, V., Mersha, T., Weirauch, M., Salomonis, N., Ryan, P., LeMasters, G.K. et al. (2017) KIF3A genetic variation is associated with pediatric asthma in the presence of eczema independent of allergic rhinitis. *J. Allergy Clin. Immunol.*, **140**, 595, e595–598.
- Marenholz, I., Esparza-Gordillo, J., Ruschendorf, F., Bauerfeind, A., Strachan, D.P., Spycher, B.D., Baurecht, H., Margaritte-Jeannin, P., Saaf, A., Kerkhof, M. et al. (2015) Meta-analysis identifies seven susceptibility loci involved in the atopic march. *Nat. Commun.*, **6**, 8804.
- Giridhar, P.V., Bell, S.M., Sridharan, A., Rajavelu, P., Kitzmiller, J.A., Na, C.L., Kofron, M., Brandt, E.B., Ericksen, M., Naren, A.P. et al. (2016) Airway epithelial KIF3A regulates Th2 responses to aeroallergens. *J. Immunol.*, **197**, 4228–4239.
- Marszalek, J.R., Ruiz-Lozano, P., Roberts, E., Chien, K.R. and Goldstein, L.S. (1999) Situs inversus and embryonic ciliary morphogenesis defects in mouse mutants lacking the KIF3A subunit of kinesin-II. *Proc. Natl. Acad. Sci. U.S.A.*, **96**, 5043–5048.
- Takeda, S., Yonekawa, Y., Tanaka, Y., Okada, Y., Nonaka, S. and Hirokawa, N. (1999) Left-right asymmetry and kinesin superfamily protein KIF3A: new insights in determination of laterality and mesoderm induction by kif3A^{-/-} mice analysis. *J. Cell Biol.*, **145**, 825–836.
- Matsuda, H., Watanabe, N., Geba, G.P., Sperl, J., Tsudzuki, M., Hiroi, J., Matsumoto, M., Ushio, H., Saito, S., Askenase, P.W. and Ra, C. (1997) Development of atopic dermatitis-like skin lesion with IgE hyperproduction in NC/Nga mice. *Int. Immunol.*, **9**, 461–466.
- Otsuka, A., Doi, H., Egawa, G., Maekawa, A., Fujita, T., Nakamizo, S., Nakashima, C., Nakajima, S., Watanabe, T., Miyachi, Y. et al. (2014) Possible new therapeutic strategy to regulate atopic dermatitis through upregulating filaggrin expression. *J. Allergy Clin. Immunol.*, **133**, 139.
- Fallon, P.G., Sasaki, T., Sandilands, A., Campbell, L.E., Saunders, S.P., Mangan, N.E., Callanan, J.J., Kawasaki, H., Shiohama, A., Kubo, A. et al. (2009) A homozygous frameshift mutation in the mouse Flg gene facilitates enhanced percutaneous allergen priming. *Nat. Genet.*, **41**, 602–608.
- Saunders, S.P., Goh, C.S., Brown, S.J., Palmer, C.N., Porter, R.M., Cole, C., Campbell, L.E., Gierlinski, M., Barton, G.J., Schneider, G. et al. (2013) Tmem79/Matt is the matted mouse gene and is a predisposing gene for atopic dermatitis in human subjects. *J. Allergy Clin. Immunol.*, **132**, 1121–1129.
- Kawasaki, H., Nagao, K., Kubo, A., Hata, T., Shimizu, A., Mizuno, H., Yamada, T. and Amagai, M. (2012) Altered stratum corneum barrier and enhanced percutaneous immune responses in filaggrin-null mice. *J. Allergy Clin. Immunol.*, **129**, 1538, e1536–1546.
- Ewald, D.A., Malajian, D., Krueger, J.G., Workman, C.T., Wang, T., Tian, S., Litman, T., Guttman-Yassky, E. and Suarez-Farinas, M. (2015) Meta-analysis derived atopic dermatitis (MADAD) transcriptome defines a robust AD signature highlighting the involvement of atherosclerosis and lipid metabolism pathways. *BMC Med. Genet.*, **8**, 60.
- Brunner, P.M., Israel, A., Leonard, A., Pavel, A.B., Kim, H.J., Zhang, N., Czarnowicki, T., Patel, K., Murphrey, M., Ramsey, K. et al. (2019) Distinct transcriptomic profiles of early-onset atopic dermatitis in blood and skin of pediatric patients. *Ann. Allergy Asthma Immunol.*, **122**, 318, e313–330.
- Matterne, U., Bohmer, M.M., Weisshaar, E., Jupiter, A., Carter, B. and Apfelbacher, C.J. (2019) Oral H1 antihistamines as 'add-on' therapy to topical treatment for eczema. *Cochrane Database Syst. Rev.*, **1**, CD012167.
- Juarez, T.M., Piccioni, D., Rose, L., Nguyen, A., Brown, B. and Kesari, S. (2021) Phase I dose-escalation, safety, and CNS pharmacokinetic study of dexanabinol in patients with brain cancer. *Neurooncol Adv*, **3**, vdab006.
- Gupta, J., Grube, E., Ericksen, M.B., Stevenson, M.D., Lucky, A.W., Sheth, A.P., Assa'ad, A.H. and Khurana Hershey, G.K. (2008) Intrinsically defective skin barrier function in children with atopic dermatitis correlates with disease severity. *J. Allergy Clin. Immunol.*, **121**, 725, e722–730.
- Gaffal, E., Glodde, N., Jakobs, M., Bald, T. and Tuting, T. (2014) Cannabinoid 1 receptors in keratinocytes attenuate fluorescein isothiocyanate-induced mouse atopic-like dermatitis. *Exp. Dermatol.*, **23**, 401–406.
- Schlosburg, J.E., Boger, D.L., Cravatt, B.F. and Lichtman, A.H. (2009) Endocannabinoid modulation of scratching response in an acute allergenic model: a new prospective neural therapeutic target for pruritus. *J. Pharmacol. Exp. Ther.*, **329**, 314–323.

29. Kwon, O.S., Kim, W., Cha, H.J. and Lee, H. (2019) In silico drug repositioning: from large-scale transcriptome data to therapeutics. *Arch. Pharm. Res.*, **42**, 879–889.
30. Möbus, L., Rodriguez, E., Harder, I., Stölzl, D., Boraczynski, N., Gerdes, S., Kleinheinz, A., Abraham, S., Heratizadeh, A., Handrick, C. et al. (2020) Atopic dermatitis displays stable and dynamic skin transcriptome signatures. *J. Allergy Clin. Immunol.*, **147**, 213–223.
31. McCauley, H.A., Liu, C.Y., Attia, A.C., Wikenheiser-Brokamp, K.A., Zhang, Y., Whitsett, J.A. and Guasch, G. (2014) TGFbeta signaling inhibits goblet cell differentiation via SPDEF in conjunctival epithelium. *Development*, **141**, 4628–4639.
32. Lin, F., Hiesberger, T., Cordes, K., Sinclair, A.M., Goldstein, L.S., Somlo, S. and Igarashi, P. (2003) Kidney-specific inactivation of the KIF3A subunit of kinesin-II inhibits renal ciliogenesis and produces polycystic kidney disease. *Proc. Natl. Acad. Sci. U.S.A.*, **100**, 5286–5291.
33. Li, B. and Dewey, C.N. (2011) RSEM: accurate transcript quantification from RNA-Seq data with or without a reference genome. *BMC Bioinformatics*, **12**, 323.
34. Risso, D., Ngai, J., Speed, T.P. and Dudoit, S. (2014) Normalization of RNA-seq data using factor analysis of control genes or samples. *Nat. Biotechnol.*, **32**, 896–902.
35. Wang, J., Vasaikar, S., Shi, Z., Greer, M. and Zhang, B. (2017) WebGestalt 2017: a more comprehensive, powerful, flexible and interactive gene set enrichment analysis toolkit. *Nucleic Acids Res.*, **45**, W130–W137.
36. Lamb, J., Crawford, E.D., Peck, D., Modell, J.W., Blat, I.C., Wrobel, M.J., Lerner, J., Brunet, J.P., Subramanian, A., Ross, K.N. et al. (2006) The connectivity map: using gene-expression signatures to connect small molecules, genes, and disease. *Science*, **313**, 1929–1935.
37. Subramanian, A., Narayan, R., Corsello, S.M., Peck, D.D., Natoli, T.E., Lu, X., Gould, J., Davis, J.F., Tubelli, A.A., Asiedu, J.K. et al. (2017) A next generation connectivity map: L1000 platform and the first 1,000,000 profiles. *Cell*, **171**, 1437, e1417–1452.
38. Wang, Y., Yella, J. and Jegga, A.G. (2019) Transcriptomic data mining and repurposing for computational drug discovery. *Methods Mol. Biol.*, **1903**, 73–95.